IEEE SENSORS JOURNAL, VOL. XX, NO. XX, XXXX 2023 1
Volume 23, Issue 19, October 2023, 23011-23019

Radar Detection Performance Via Frequency Agility Using Measured UAVs RCS Data

Massimo Rosamilia, *Member, IEEE*, Augusto Aubry, *Senior Member, IEEE*, Alessio Balleri, Vincenzo Carotenuto, *Senior Member, IEEE*, and Antonio De Maio, *Fellow, IEEE*

***Abstract*— This paper addresses radar detection performance prediction (via measured data) for drone targets using a frequency agility-based incoherent (square-law) detector. To this end, a preliminary statistical analysis of the integrated Radar Cross Section (RCS) resulting from frequency agile pulses is carried out for drones of different sizes and characteristics, using data acquired in a semi-controlled environment for distinct frequencies, angles, and polarizations. The analysis involves fitting the integrated RCS measurements with commonly used one-parametric and two-parametric probability distributions and leverages the Cramér-von Mises distance and the Kolmogorov Smirnov test. Results show that the Gamma distribution appears to accurately model the resulting fluctuations. Hence, the impact of integration and frequency agility on the RCS fluctuation dispersion is studied. Finally, detection performance of the incoherent square-law detector is assessed for different target and radar parameters, using both measured and simulated data drawn from a Gamma distribution whose parameters follow the preliminary RCS statistical analysis. The results highlight a good agreement between simulated and measurement-based curves.**

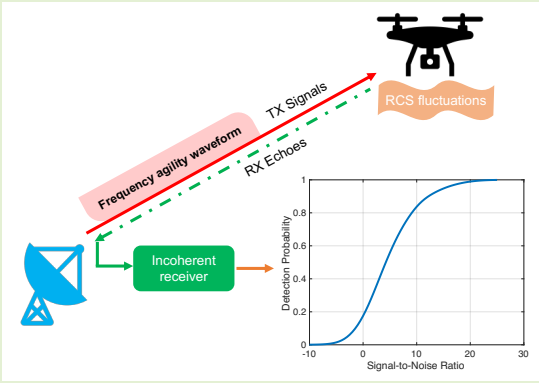

I. Introduction

In recent years, Unmanned Aerial Vehicles (UAVs), commonly referred to as drones, have become increasingly popular in both commercial and military applications. However, the use of drones has raised privacy and security concerns, especially when they are used for nefarious purposes. Thus, the need for effective surveillance systems has become more pressing than ever before. However, due to their small size and low Radar Cross Section (RCS), drones pose a significant challenge to the radar detection task. As a result, in the open literature significant effort has been devoted to the study of drone RCS signatures and their impact on radar performance. As a matter of fact, [1] focused on the RCS measurements of small UAVs for different aspect angles in the frequency interval 8-12 GHz and in VV polarization. Then, resorting to the inverse synthetic aperture radar method, an accurate analysis of the main drone scattering components has been provided. In [2], the drone RCS data have been collected in the frequency interval 26-40 GHz, whereas in [3], the RCS of two off-the-shelf UAVs has been collected in the frequency range 5.8-8.2 GHz. Drone signatures in the Ku-band have been collected in [4], whereas 3D RCS data of a nano-drone between 23 GHz and 25 GHz have been collected in [5]. Moreover, RCS data of some nano and micro drones in the X-band have been collected in [6] for several elevation angles, providing some statistical features related to the measured dataset. The authors of [7] carried out a statistical analysis of the RCS signatures and presented a specific UAV recognition performance analysis whereas [4] analyzed the detection performance in a short-range battlefield context. In [8], experiments using a 35 GHz Frequency Modulated Continuous Wave (FMCW) radar has been conducted for small UAV-detection, whilst, in [9], the imaging MIMO MIRA-CLE Ka system has been employed to investigate drone detection performance. In [10], using an experimental X-band FMCW radar, DJI-Phantom 4 RCS data have been collected to assess detection performance, whereas other discussions on UAV detection via FMCW radars can be found in [11]. In addition, the problem of UAV payload classification has been addressed in [12] exploiting micro-Doppler signatures, whereas the detection and localization of UAV swarms have been studied in [13] and [14], leveraging gridless sparse techniques. Furthermore, [15] has offered a literature review of drone activity monitoring using radars. Last but not least, in [16] the RCSs of several drones have been statistically analyzed and then, in the context of a coherent detection, the radar detection performance has been studied

Massimo Rosamilia is with the National Inter-University Consortium for Telecommunications, 43124 Parma, Italy (e-mail: massimo.rosamilia@unina.it).

Augusto Aubry, Vincenzo Carotenuto, and Antonio De Maio are with Università degli Studi di Napoli "Federico II", DIETI, Via Claudio 21, I-80125 Napoli, Italy, and also with the National Inter-University Consortium for Telecommunications, 43124 Parma, Italy (e-mail: augusto.aubry@unina.it; vincenzo.carotenuto@unina.it; ademaio@unina.it). (Corresponding author: Antonio De Maio)

Alessio Balleri is with the Centre for Electronic Warfare, Information and Cyber, Cranfield University, Defence Academy of the United Kingdom, Shrivenham, SN6 8LA (email: a.balleri@cranfield.ac.uk).

with respect to the integrated Signal-to-Noise Ratio (SNR) at the radar receiver, assuming a non-fluctuating RCS over each Coherent Processing Interval (CPI).

Notably, one approach to mitigate the effects of RCS fluctuations is the employment of an incoherent pulse-to-pulse integration leveraging frequency agility technique, which induce some diversity of the target RCS within a given CPI by transmitting pulses at different frequencies [17]. In the open literature, such strategy has been successfully applied to multi-target parameter estimation [18] and target detection [19]–[23].

In this context, the aim of this paper is to extend the work presented in [16] and study the performance of the square-law incoherent detector using frequency agility to establish the presence of drone targets leveraging measured data. Towards this goal, a statistical analysis of the integrated RCS resulting from frequency agile pulses is conducted for several UAVs of different sizes and characteristics. The considered dataset has been introduced in [16], which includes measurements of the AscTec Firefly, AscTec Pelican, Venom VN10, Parrot AR.DRONE, and DJI Matrice 100, acquired in a semi-controlled environment for different frequencies (in the range 8.2-18 GHz), polarizations (HH and VV), and azimuth aspect angles (in the interval 0-360 degrees).

To analyze the resulting incoherent RCS sum, some one-parametric and two-parametric probability distributions (commonly used to model RCS fluctuations) are considered. Hence, the Cramér-von Mises (CVM) distance and the Kolmogorov–Smirnov (KS) test are employed to evaluate the goodness-of-fit of the considered distributions. The results show that a bespoke Gamma distribution is capable of accurately modeling such fluctuations provided that its parameters are tailored to the drone type, frequency hopping step, and polarization. Moreover, the dispersion of RCS fluctuations is studied versus the number of integrated pulses and frequency agility step. Finally, the detection performance of the (square-law) incoherent detector exploiting frequency agility is evaluated using both the measured data and the theoretical Gamma model (with distributional parameters inferred from the measurements) for different operational scenarios, including varying frequency hopping steps and number of pulses.

The rest of the paper is organized as follows. Section II provides an overview of the experimental setup and the pre-processing steps used for data acquisition. The statistical behavior of the integrated measured RCS is studied in Section III, while the radar detection performance is evaluated in Section IV. Finally, Section V addresses concluding remarks and outlines some possible future research avenues.

II. Measurements Setup

This section provides a brief description of the test-bed and the data processing steps used to measure the drone RCS (the interested reader may refer to [16] for further details).

The RCS data have been collected in a semi-controlled environment by means of a 2-port Vector Network Analyzer (VNA) equipped with a pair of identical standard horn antennas (one on transmit and the other one on receive) and a fully controlled turntable, which provided an angular step resolution of 0.1 degrees (see Fig. 1). Five drones with different shapes and dimensions (see Table I and Fig. 2) have been analyzed in the frequency interval 8.2-18 GHz, in both HH and VV polarizations, for 3600 different aspect angles and elevation close to 0°.

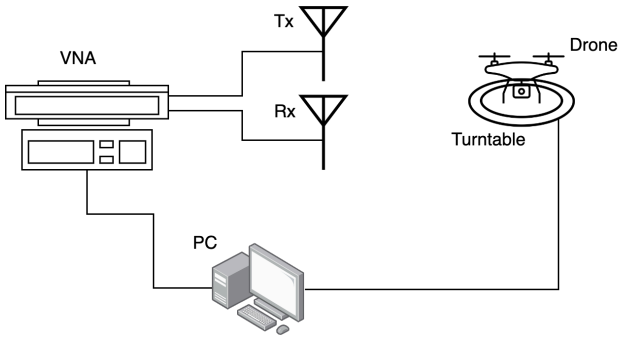

Fig. 1: Notional representation of the experimental setup.

The RCS data acquisition process involves coherent background subtraction and range-gating (employing a tailored rectangular window) operations to obtain a clean high range resolution target response. Then, the frequency spectrum of the resulting signal is computed and the point-like response of the target is extracted considering a moving bandwidth of 40 MHz. Hence, for a given polarization and central frequency (in the measured X and Ku bands), the squared magnitude peak in the time domain is obtained, which corresponds to the non-calibrated target RCS. Therefore, using the substitution method [24] with a 10 cm diameter calibrating sphere, the aforementioned value is appropriately scaled and the absolute RCS of the target is computed. Thus, for each analyzed UAV, the process is repeated for all the aspect angles of interest considering different central frequencies and polarizations. More details can be found in [16].

III. Statistical Analysis

To provide accurate drone detection performance prediction using a frequency agile radar, a statistical characterization of the integrated RCS fluctuations versus the azimuth aspect angle is essential. To this end, denoting by $\sigma(\theta, f, P)$ the drone RCS for azimuth θ, frequency f, and polarization $P \in \{HH, VV\}$, the integrated RCS, assuming N pulses, frequency hopping step Δf, and starting frequency f_0, is given by

$$\tilde{\sigma}(\theta, f_0, \Delta f, N, P) = \sum_{i=1}^{N} \sigma(\theta, f_i, P), \tag{1}$$

where $f_i = f_0 + (i-1)\Delta f$. This is a very important parameter as it rules the performance of the square law incoherent detector [17], [25], [26].

In the following, a statistical analysis of the integrated RCS measurements (1) of the five drones listed in Table I is thus carried out, following the same line of reasoning as in [16] which deals with the case of a single frequency RCS measurement. In particular, a first-order statistical analysis is performed by fitting (1) with (one-parametric and two-parametric) distributions typically employed to model fluctuations [17], such as the

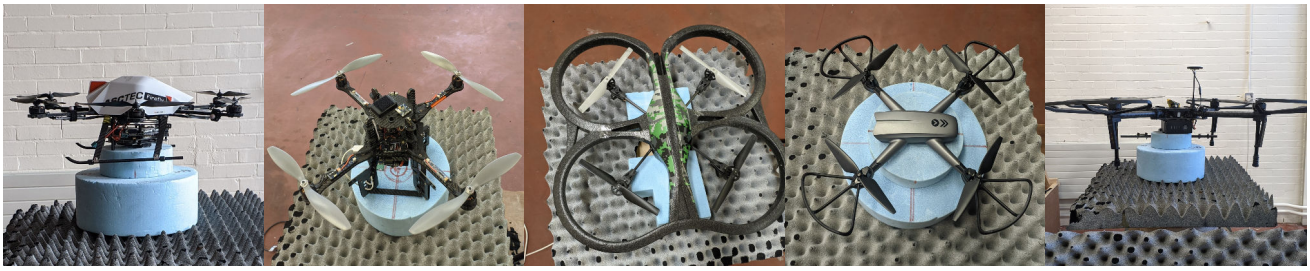

(a) (b) (c) (d) (e)

Fig. 2: Measured drones: (a) AscTec Firefly (b) AscTec Pelican (c) Parrot AR.DRONE 2.0 (d) Venom VN10 (e) DJI Matrice 100.

TABLE I: Measured Drones Specifications.

Drone	# Rotors	Weight	Width	Depth	Height
AscTec Firefly	6	1600 g	470 mm	430 mm	165 mm
AscTec Pelican	4	1650 g	360 mm	360 mm	188 mm
Parrot AR.DRONE 2.0	4	420 g	517 mm	517 mm	127 mm
Venom VN10	4	148 g	290 mm	210 mm	38 mm
DJI Matrice 100	4	2355 g	759 mm	755 mm	205 mm

Exponential, Log-Normal, Weibull, and Gamma distributions. The parameter vector of the distributions is determined via the minimization of the CVM distance [27] between the empirical and the theoretical Cumulative Distribution Functions (CDFs), i.e., as a solution to the following optimization problem [16]

$$\widehat{\boldsymbol{\theta}}(f_0, \Delta f, N, P) = \arg\min_{\boldsymbol{\theta}} CVM\left(\hat{\boldsymbol{\sigma}}(f_0, \Delta f, N, P), F(x; \boldsymbol{\theta})\right), \tag{2}$$

where $F(x;\boldsymbol{\theta})$ is the CDF of the distribution under test, $\boldsymbol{\theta}$ denotes the vector whose entries are the distributional parameters,

$$\begin{aligned}&\hat{\boldsymbol{\sigma}}(f_0, \Delta f, N, P)\\ &= [\tilde{\sigma}(\theta_1, f_0, \Delta f, N, P), \tilde{\sigma}(\theta_2, f_0, \Delta f, N, P),\\ &\quad \ldots, \tilde{\sigma}(\theta_n, f_0, \Delta f, N, P)]^{\mathrm{T}} \in \mathbb{R}^n\end{aligned} \tag{3}$$

is the vector of the integrated RCS measurements observed at the aspect angles $\theta_i \in \{(i-1)/10\}$ degrees, $i = 1, \ldots, n$, with $n = 3600$, and [27]

$$\begin{aligned}&CVM(\hat{\boldsymbol{\sigma}}(f_0, \Delta f, N, P), F(x; \boldsymbol{\theta}))\\ &= \sqrt{\frac{1}{12n} + \sum_{i=1}^{n}\left[\frac{2i-1}{2n} - F(\tilde{\sigma}(\theta_i, f_0, \Delta f, N, P); \boldsymbol{\theta})\right]^2}\end{aligned} \tag{4}$$

is the CVM distance, with $(\cdot)^{\mathrm{T}}$ being the transpose operator and $\mathbb{R}^N$ the set of N-dimensional column vectors of real numbers. The optimization problem in (2) is tackled by means of the iterative algorithm proposed in [28] which is implemented in MATLAB with the function *fminsearch* using, as initial estimates of the distributional parameters, those obtained via the MATLAB function *fitdist*.

Then, the most appropriate statistical model is selected by examining the CVM distance and the KS test results. As a matter of fact, the KS is a non parametric statistical procedure which can be used to assess the goodness-of-fit between the empirical and the theoretical RCS distributions [27], [29].

According to the obtained CVM distances, reported in Table II for the AscTec Firefly's integrated RCS at $f_0 = 13$ GHz, the Gamma model accurately describes RCS fluctuations, achieving in general the lowest average CVM distance, while the Weibull distribution often ranks second. In particular, for $N = 8$ pulses, the Weibull distribution reaches CVM distances close to the Gamma model. Notably, unlike the Weibull, the Gamma fluctuation law can enable a closed-form analytical evaluation of the detection performance [30]. The KS test results unveils that, independently of the drone, in all the analyzed cases the hypothesis that the data are distributed according to the Gamma distribution cannot be rejected (significance level $\alpha_{KS} = 0.01$) [31]. It is also interesting to observe that the statistical analysis reveals that the shape parameter ν of the fitted Gamma model, illustrated in Fig. 3 with regard to the AscTec Firefly at $f_0 = 13$ GHz, increases with the number of pulses, regardless of the drone type, carrier frequency, and polarization. Indeed, as the number of pulses increases, the integrated RCS becomes more and more concentrated around the mean value. Furthermore, not surprisingly, the shape parameter also increases with the frequency hopping step for a given number of pulses, because increasing the frequency leads to higher and higher RCS decorrelation.

Single frequency RCS and integrated RCS (both normalized to their maximum value) of AscTec Firefly for $f_0 = 13$ GHz and HH polarization are compared in Fig. 4. Specifically, single frequency RCS is displayed in Fig. 4 (a) whereas, assuming $N = 16$ pulses, integrated RCS for $\Delta f = 15$ MHz and $\Delta f = 45$ MHz are illustrated in Figs. 4 (b) and (c), respectively. The plots clearly unveil the reduced RCS fluctuations achieved with the frequency-agility technique. In particular, it is worth noting that the normalized single frequency RCS measurement can reach values below 10^{-3}, whereas the integrated RCS dynamic range becomes more and more compact as the frequency hopping step increases. As a

TABLE II: CVM distances between empirical and theoretical CDF of AscTec Firefly's integrated RCS at $f_0 = 13$ GHz at varying polarization, frequency hopping steps, and numbers of pulses.

HH pol	$N = 8$ pulses			$N = 16$ pulses		
Distribution	$\Delta f = 15$ MHz	$\Delta f = 30$ MHz	$\Delta f = 45$ MHz	$\Delta f = 15$ MHz	$\Delta f = 30$ MHz	$\Delta f = 45$ MHz
Exponential	0.61	1.73	2.87	1.77	3.86	5.42
Gamma	**0.27**	**0.51**	**0.80**	**0.51**	1.15	1.11
LogNormal	2.37	1.94	1.47	1.95	**0.98**	**0.70**
Weibull	0.28	0.56	0.96	0.56	1.42	1.67
VV pol	$N = 8$ pulses			$N = 16$ pulses		
Distribution	$\Delta f = 15$ MHz	$\Delta f = 30$ MHz	$\Delta f = 45$ MHz	$\Delta f = 15$ MHz	$\Delta f = 30$ MHz	$\Delta f = 45$ MHz
Exponential	1.61	2.41	3.26	2.39	4.44	6.49
Gamma	0.47	**0.39**	**0.76**	**0.41**	**1.07**	**0.76**
LogNormal	2.66	1.99	1.44	1.94	1.08	1.31
Weibull	**0.34**	0.64	1.14	0.66	1.63	1.66

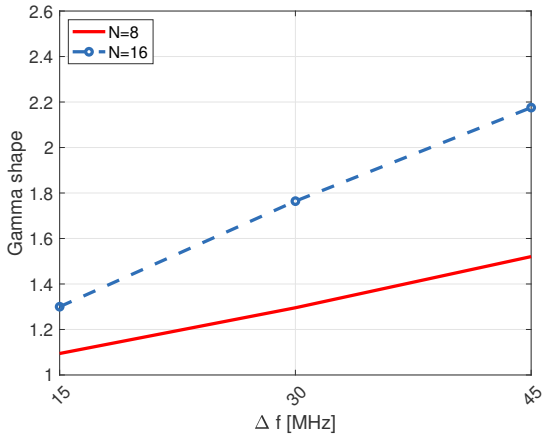

(a)

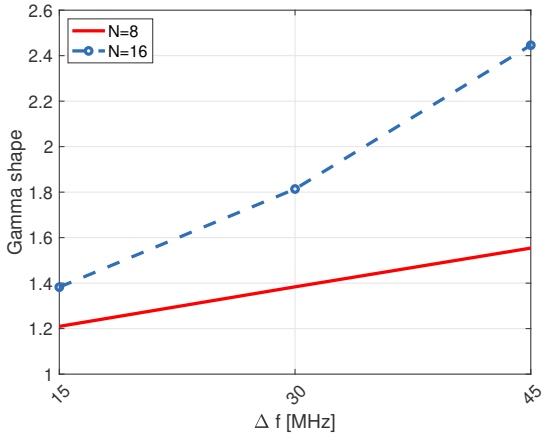

(b)

Fig. 3: Analysis of the Gamma shape parameter ν versus frequency hopping step for two values of the number of pulses, i.e., $N = \{8, 16\}$. The Gamma shape parameters are fitted with the RCS measurements of AscTec Firefly at $f_0 = 13$ GHz and (a) HH polarization, (b) VV polarization.

matter of fact, assuming $N = 16$ pulses and $\Delta f = 15$ MHz, i.e., the situation of Fig. 4 (b), the normalized integrated RCS values belong to the range $[10^{-3}, 1]$, whereas for the case of Fig. 4 (c), i.e., $N = 16$ pulses and $\Delta f = 30$ MHz, the range of values is further reduced, namely $[10^{-2}, 1]$.

To further shed light on the effect of frequency agility on the resulting RCS, in Table III, two scale-invariant dispersion score indicators (a measure of how spread is a dataset) are provided: the Pearson Coefficient of Dispersion (PCOD) (also known as coefficient of variation) [32] and the Quartile Coefficient of Dispersion (QCOD) [33], computed using the Asctec Firefly measured data at $f_0 = 13$ GHz. They are reported for different numbers of pulses and frequency hopping steps. In particular, the PCOD and the QCOD are defined as

$$\text{PCOD} = \frac{\hat{S}}{\hat{\mu}} \tag{5}$$

and

$$\text{QCOD} = \frac{Q_3 - Q_1}{Q_3 + Q_1} \tag{6}$$

respectively, with the involved statistics computed from the observations of integrated RCS at varying azimuth aspect angles, i.e.,

- $\hat{S}$ the sample standard deviation;
- $\hat{\mu}$ the sample mean;
- Q_1 the first sample quartile;
- Q_3 the third sample quartile.

The reported results clearly show that, regardless of the considered polarization and the employed frequency hopping step, integrating the RCS results in a dispersion that is smaller and smaller as the number of pulses increases. Moreover, as expected, the inspection of the table reveals that, for a given number of pulses, the dispersion of RCS fluctuations is reduced by increasing the frequency agility step, due to the higher and higher RCS diversity. It is worth pointing out that a different estimate for the PCOD leveraging the theoretical fitting Gamma distribution can be conceived (PCOD_t). It just requires the knowledge of the fitting Gamma distribution shape parameter (available in Fig. 3), and can be computed as

$$PCOD_t = \frac{1}{\sqrt{\nu}}. \tag{7}$$

Although the numerical values of the PCOD_t are not reported here to avoid redundancy, the above considerations about RCS dispersion are robust with respect to the chosen PCOD estimation procedure. Furthermore, this trend holds considering both PCOD and QCOD metrics, namely both the performance indices support the obtained results.

As a final remark, despite the results presented in Table III are related to the observation of the Asctec Firefly (which in this work is considered as a sample study case), the dispersion

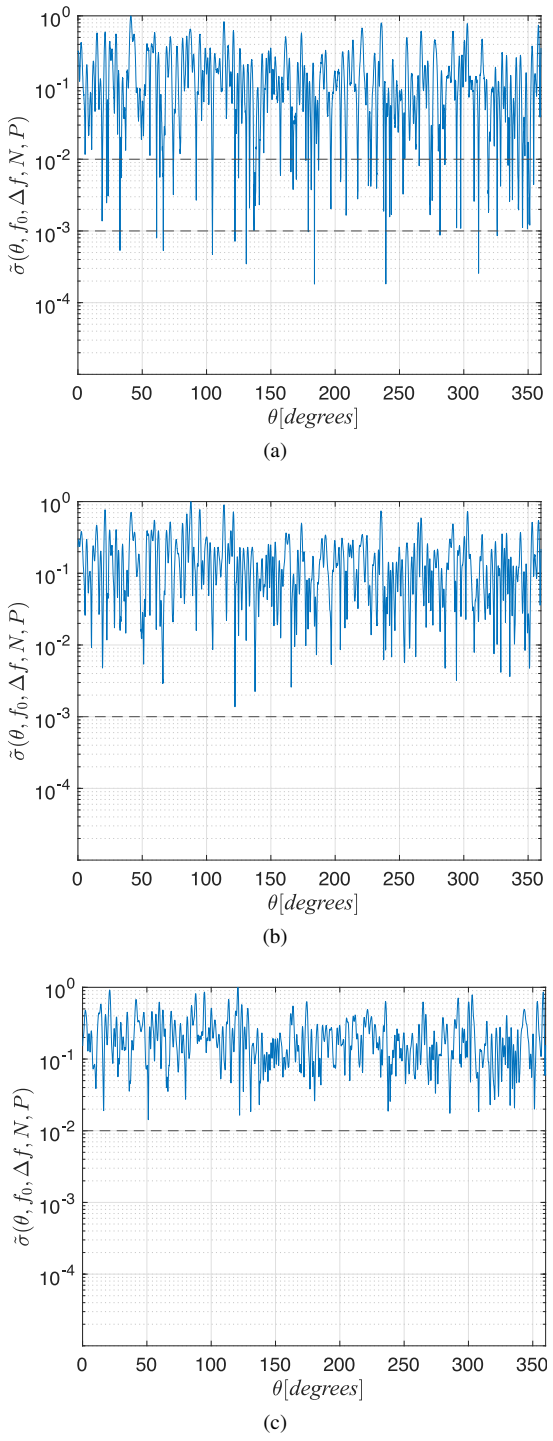

Fig. 4: AscTec Firefly integrated RCS (normalized to the maximum value), for $f_0 = 13$ GHz and HH polarization. (a) $N = 1$, (b) $N = 16$, $\Delta f = 15$ MHz, and (c) $N = 16$, $\Delta f = 45$ MHz.

fluctuation trend also holds for the other considered UAVs and carrier frequencies (see e.g., the results reported in Table IV for the case of $N = 8$, $f_0 = 13$ GHz, and HH polarization). In general, repeating the analysis of this section with the measured data from the other drones listed in Table I and for different frequencies, similar RCS fluctuation characteristics are experienced.

TABLE III: PCOD and QCOD using measured AscTec Firefly RCS for $N = \{1, 8, 16\}$, $\Delta f = \{15, 30, 45\}$ MHz, and $f_0 = 13$ GHz.

		PCOD		QCOD	
N	Δf **MHz**	HH	VV	HH	VV
1	-	0.999	0.908	0.656	0.625
8	15	0.964	0.875	0.640	0.608
8	30	0.914	0.866	0.606	0.561
8	45	0.854	0.863	0.571	0.530
16	15	0.913	0.871	0.605	0.561
16	30	0.796	0.820	0.522	0.481
16	45	0.723	0.682	0.462	0.409

Summarizing, the analysis presented in this section clearly corroborates the benefits of employing frequency agile techniques to counter the UAV RCS fluctuation.

IV. Detection Performance Analysis

In this section, the detection capabilities of the incoherent square-law receiver are analyzed by comparing the performance obtained under measured integrated target RCS fluctuations with that resulting from an appropriate statistical model using different carrier frequencies f_0, frequency hopping steps Δf, and number of pulses N. The Probability of detection (P_d), computed assuming a desired Probability of false alarm $P_{fa} = 10^{-4}$, is used as performance metric. Moreover, due to the unavoidable fluctuations in the integrated RCS and hence in the resulting SNR of the received radar signal, the performance is extremely dependent on the aspect angle. This poses a problem in the evaluation of the radar detection probability because its exact computation for each aspect angle is both complicated and of no practical utility (a perfect knowledge/estimate of the target aspect angle is reasonably unavailable) [17]. Therefore, an average performance based on a statistical framework for the integrated RCS (modeled as a random variable, being subsumed random the aspect angle) is a viable means to carry out a detection analysis [34]–[36].

In the following, let us consider a frequency agile radar illuminating the target using N pulses at frequency $f_i = f_0 + (i-1)\Delta f$, $i = 1, \ldots, N$. Let us also assume that the azimuth aspect angle of the drone is constant within the radar processing interval. Notably, due to the employed frequency shift in the transmitted pulses and the UAV size, a decorrelation between the target RCS measurements at each pulse is expected. Assuming polarization $P \in \{HH, VV\}$, the radar sample collected from the range bin of interest and the i-th pulse can be modeled as

$$z_i = \sqrt{\tilde{\sigma}(\theta, f_i, P)} e^{j\phi_i} + n_i, \; i = 1, \ldots, N \tag{8}$$

where

- ϕ_i accounts for the unknown UAV phase response at the i-th pulse;
- $n_i \sim \mathcal{CN}(0, \sigma_n^2)$, $i = 1, \ldots, N$, are independent and identically distributed (IID) zero-mean, circularly symmetric, Gaussian noise samples with unknown variance σ_n^2 .

TABLE IV: PCOD and QCOD using measured drones RCS for $N = 8$, $\Delta f = \{15, 30, 45\}$ MHz, $f_0 = 13$ GHz, and HH polarization.

	PCOD			QCOD		
Drone	$\Delta f = 15$ MHz	$\Delta f = 30$ MHz	$\Delta f = 45$ MHz	$\Delta f = 15$ MHz	$\Delta f = 30$ MHz	$\Delta f = 45$ MHz
AscTec Firefly	0.964	0.914	0.854	0.640	0.606	0.571
AscTec Pelican	1.199	1.189	1.179	0.680	0.674	0.656
Parrot AR.DRONE 2.0	0.880	0.844	0.797	0.608	0.574	0.528
Venom VN10	0.957	0.918	0.857	0.613	0.575	0.527
DJI Matrice 100	1.315	1.172	1.038	0.653	0.575	0.498

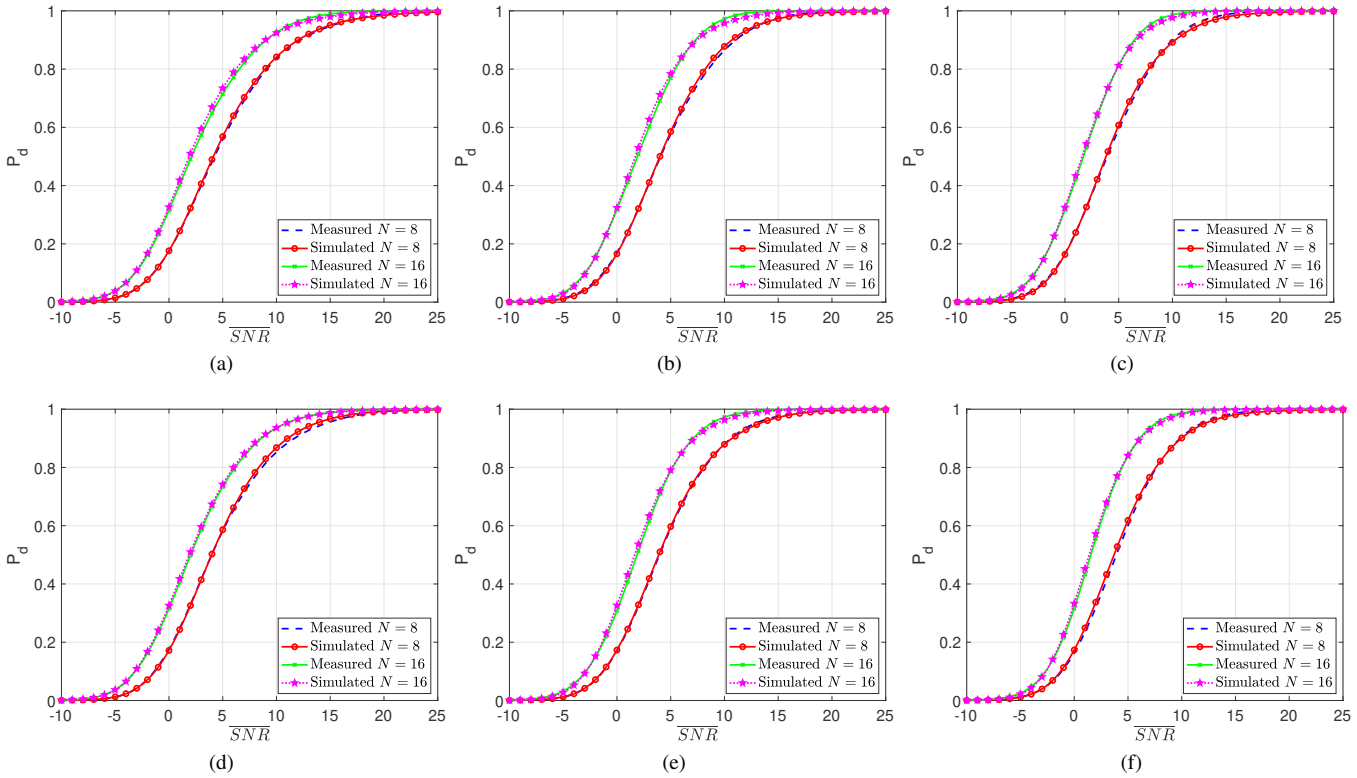

Fig. 5: P_d curves versus $\overline{SNR}$ using measured and simulated AscTec Firefly RCS for two number of pulses, i.e., $N = \{8, 16\}$, $f_0 = 13$ GHz, and: (a) and (d) $\Delta f = 15$ MHz, (b) and (e) $\Delta f = 30$ MHz, (c) and (f) $\Delta f = 45$ MHz. Moreover, HH is considered in (a), (b), and (c); VV in (d), (e), and (f).

Therefore, let us consider the incoherent square-law detector [17]

$$z = \sum_{i=1}^{N} |z_i|^2 \underset{\mathcal{H}_0}{\overset{\mathcal{H}_1}{\gtrless}} \zeta, \tag{9}$$

where $\mathcal{H}_0$ and $\mathcal{H}_1$ indicate the null and the alternative hypothesis (i.e., target echo absence/presence within the received observation vector), respectively, and ζ is the detection threshold set to ensure the desired P_{fa}. Precisely, for the case at hand, the P_{fa} is given by [25]

$$P_{fa} = e^{-\zeta} \sum_{i=0}^{N-1} \frac{\zeta^i}{i!}. \tag{10}$$

To proceed further, let us denote by $\overline{SNR}$ the average single-pulse SNR over all aspect angles, the P_d for the decision rule in (9) at the aspect angle θ can be obtained as [25][1]

$$P_d(\overline{SNR}, \theta, f_0, \Delta f, N, P) = Q_N\left(\sqrt{2N\overline{SNR}\frac{\tilde{\sigma}(\theta, f_0, \Delta f, N, P)}{\bar{\sigma}(f_0, \Delta f, N, P)}}, \sqrt{2\zeta}\right) \tag{11}$$

with $\bar{\sigma}(f_0, \Delta f, N, P)$ the sample mean (over aspect angle) target integrated RCS value and $Q_N(\cdot, \cdot)$ the generalized Marcum Q-function of N-th order [30]. Hence, the empirical average detection performance over the aspect angle can be computed as

$$P_d(\overline{SNR}, f_0, \Delta f, N, P) = \frac{1}{3600}\sum_{\theta \in \mathbb{T}} P_d(\overline{SNR}, \theta, f_0, \Delta f, N, P), \tag{12}$$

[1]Notice that the performance analysis can be extended to the case of non-Gaussian clutter. Specifically, the computation procedure remains the same; however, it requires the utilization of the specific conditional P_d tied up to the clutter statistical properties.

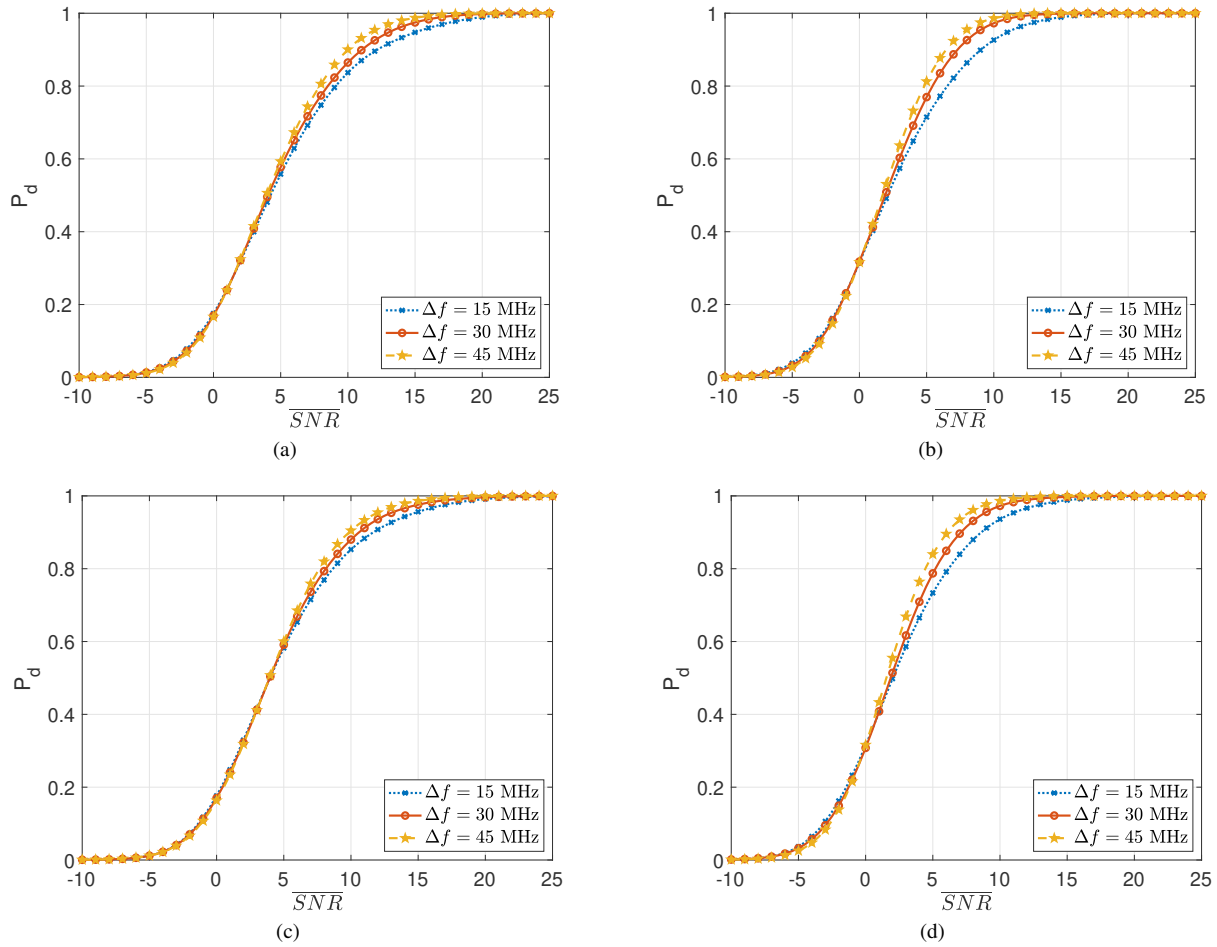

Fig. 6: P_d curves versus $\overline{SNR}$ using measured AscTec Firefly RCS for three different frequency hopping steps, i.e., $\Delta f = \{15, 30, 45\}$ MHz, $f_0 = 13$ GHz, and: (a) and (c) $N = 8$, (b) and (d) $N = 16$. Moreover, HH is considered in (a) and (b); VV in (c) and (d).

where $\mathbb{T} = \{i \times 0.1,\ i = 0, \ldots, 3599\}$.

To corroborate the Gamma fluctuation model inferred in Section III also from a radar detection point of view, the resulting average P_d for the theoretical Gamma distribution is considered too. Specifically, it is computed as

$$P_d(\overline{SNR}, f_0, \Delta f, N, P) = \frac{1}{3600} \sum_{n=1}^{3600} Q_N \left(\sqrt{2N\overline{SNR} \frac{\rho_n(f_0, \Delta f, N, P)}{\mu(f_0, \Delta f, N, P)}}, \sqrt{2\zeta} \right), \quad (13)$$

where $\rho_n(f_0, \Delta f, N, P)$ are independent realizations of a Gamma distribution with parameter vector $\boldsymbol{\theta}(f_0, \Delta f, N, P) = [\nu(f_0, \Delta f, N, P), \beta(f_0, \Delta f, N, P)]^{\mathrm{T}}$ inferred from the fitting process, whereas $\mu(f_0, \Delta f, N, P)$ denotes the learned expected value, i.e., $\mu(f_0, \Delta f, N, P) = \nu(f_0, \Delta f, N, P)\, \beta(f_0, \Delta f, N, P)$.

P_d versus $\overline{SNR}$, related to the AscTec Firefly and $f_0 = 13$ GHz is displayed in Fig. 5, assuming $N \in \{8, 16\}$ pulses and for three different frequency hopping values, i.e., $\Delta f = 15$ MHz in Figs. 5 (a) and (d), $\Delta f = 30$ MHz in Figs. 5 (b) and (e), and $\Delta f = 45$ MHz in Figs. 5 (c) and (f). Furthermore, Figs. 5 (a), (b), and (c) refer to the HH polarization, whereas the VV polarization is considered in Figs. 5 (d), (e), and (f).

The curves show nearly perfect adherence (with negligible displacements) between the P_d obtained using measured and simulated data in all the reported study cases, proving that, also from a radar detection standpoint, the fitted Gamma distribution is capable of capturing the RCS fluctuation phenomena.

The results pinpoint that, for a given value of Δf, increasing the number of pulses leads to better and better detection performance, as the average integrated SNR experiences incoherent gain and the integrated RCS becomes more and more concentrated while growing the number of frequency hopping steps. Furthermore, for a given $\overline{SNR}$ value and number of pulses, similar P_d levels are achieved regardless of the adopted polarizations. This is not surprising and agrees with the results available in the open literature where it is reported that similar average drone RCS values are obtained in both the HH and VV polarizations [1], [16].

In Fig. 6, the P_d curves vs $\overline{SNR}$, obtained using the measured data of the AscTec Firefly drone for $f_0 = 13$ GHz and both polarizations, are reported varying the frequency hopping within $\Delta f = \{15, 30, 45\}$ MHz. The case of $N = 8$ pulses is shown in Figs. 6 (a) and (c), while the case of $N = 16$

pulses is analyzed in Figs. 6 (b) and (d).

The results highlight that in all the analyzed scenarios, for a fixed number of pulses and under the high $\overline{SNR}$ regime, an increase in the frequency agility parameter Δf leads to a performance improvement. Still, this is due to the more concentrated nature of the integrated RCS fitting distribution when a stronger frequency diversity is employed. Additionally, it appears that similar achievements are reached regardless of the considered polarization. Finally, it is worth mentioning that the behaviors pinpointed in Figs. 5 and 6 are also observed for other carrier frequencies and for the other drones (listed in Table I). This further corroborates that:

- the Gamma model is suitable to describe and capture the fluctuations in drones RCS when frequency agility techniques are employed;
- the use of frequency agility effectively mitigates the RCS fluctuation impairments, leading to a UAVs detectability boost at the high SNR regime.

V. Conclusions

In this paper a performance analysis on the effectiveness of frequency agility techniques to enhance the radar detection capabilities of drones has been conducted by leveraging measured RCS data. Specifically, based on the statistical analysis of measured drone integrated RCSs resulting from frequency agile pulses, the Gamma distribution (with parameters inferred from the acquired data) has been established as a suitable model for the description of the intrinsic UAV RCS fluctuations. Then, the performance of the incoherent square-law detector has been assessed using both measured and simulated data (whose parameters are set via the fitted Gamma model) for distinct operational scenarios, with different frequency hopping steps, polarizations, and number of pulses. The results have highlighted that frequency diversity can mitigate RCS fluctuation and there is a good agreement between Gamma simulated and measurements-based P_d curves. This pinpoints the important role of the presented analysis as a reliable means for performance prediction and appropriate system sizing/designing.

As possible future research avenues, it is worth mentioning the analysis for some other values of the elevation angle as well as the effect on RCS fluctuation and detection performance of a joint integration in frequency and polarization domains.

References

[1] M. Pieraccini, L. Miccinesi, and N. Rojhani, "RCS measurements and ISAR images of small UAVs," *IEEE Aerosp. Electron. Syst. Magazine*, vol. 32, no. 9, pp. 28–32, 2017.

[2] V. Semkin, J. Haarla, T. Pairon, C. Slezak, S. Rangan, V. Viikari, and C. Oestges, "Analyzing radar cross section signatures of diverse drone models at mmWave frequencies," *IEEE Access*, vol. 8, pp. 48 958–48 969, 2020.

[3] A. Herschfelt, C. R. Birtcher, R. M. Gutierrez, Y. Rong, H. Yu, C. A. Balanis, and D. W. Bliss, "Consumer-grade drone radar cross-section and micro-doppler phenomenology," in *2017 IEEE Radar Conference (RadarConf)*, 2017, pp. 0981–0985.

[4] J. Ochodnický, Z. Matousek, M. Babjak, and J. Kurty, "Drone detection by Ku-band battlefield radar," in *2017 International Conference on Military Technologies (ICMT)*, 2017, pp. 613–616.

[5] A. Balleri, "Measurements of the radar cross section of a nano-drone at K-band," in *2021 IEEE 8th International Workshop on Metrology for AeroSpace (MetroAeroSpace)*, 2021, pp. 283–287.

[6] P. Sedivy and O. Nemec, "Drone RCS statistical behaviour," *STO-MP-MSG-SET-183*, 2021.

[7] M. Ezuma, C. K. Anjinappa, M. Funderburk, and I. Guvenc, "Radar cross section based statistical recognition of UAVs at microwave frequencies," *IEEE Trans. Aerosp. Electron. Syst.*, vol. 58, no. 1, pp. 27–46, 2022.

[8] J. Drozdowicz, M. Wielgo, P. Samczynski, K. Kulpa, J. Krzonkalla, M. Mordzonek, M. Bryl, and Z. Jakielaszek, "35 GHz FMCW drone detection system," in *2016 17th International Radar Symposium (IRS)*, 2016, pp. 1–4.

[9] J. Klare, O. Biallawons, and D. Cerutti-Maori, "Detection of UAVs using the MIMO radar MIRA-CLE Ka," in *Proceedings of EUSAR 2016: 11th European Conference on Synthetic Aperture Radar*, 2016, pp. 1–4.

[10] A. D. de Quevedo, F. I. Urzaiz, J. G. Menoyo, and A. A. López, "Drone detection and radar-cross-section measurements by RAD-DAR," *IET Radar, Sonar & Navigation*, vol. 13, no. 9, pp. 1437–1447, 2019.

[11] M. Caris, W. Johannes, S. Sieger, V. Port, and S. Stanko, "Detection of small UAS with W-band radar," in *2017 18th International Radar Symposium (IRS)*, 2017, pp. 1–6.

[12] L. Pallotta, C. Clemente, A. Raddi, and G. Giunta, "A feature-based approach for loaded/unloaded drones classification exploiting micro-doppler signatures," in *2020 IEEE Radar Conference (RadarConf20)*, 2020, pp. 1–6.

[13] J. Zheng, R. Chen, T. Yang, X. Liu, H. Liu, T. Su, and L. Wan, "An efficient strategy for accurate detection and localization of uav swarms," *IEEE Internet of Things Journal*, vol. 8, no. 20, pp. 15 372–15 381, 2021.

[14] T. Yang, J. Zheng, T. Su, and H. Liu, "Fast and robust super-resolution doa estimation for uav swarms," *Signal Processing*, vol. 188, p. 108187, 2021.

[15] C. Clemente, F. Fioranelli, F. Colone, and G. Li, *Radar Countermeasures for Unmanned Aerial Vehicles*. London: IET, 2021.

[16] M. Rosamilia, A. Balleri, A. De Maio, A. Aubry, and V. Carotenuto, "Radar detection performance prediction using measured UAVs RCS data," *IEEE Transactions on Aerospace and Electronic Systems*, Early Access, 2022.

[17] M. A. Richards, J. A. Scheer, and W. A. Holm, *Principles of Modern Radar: Basic Principles, Volume 1*. Institution of Engineering and Technology, 2010.

[18] W. Xing, C. Zhou, and C. Wang, "Modified omp method for multi-target parameter estimation in frequency-agile distributed mimo radar," *Journal of Systems Engineering and Electronics*, vol. 33, no. 5, pp. 1089–1094, 2022.

[19] K. Horn and N. Wallace, "Detection of slowly fading targets with frequency agility," *Proceedings of the IEEE*, vol. 57, no. 5, pp. 817–818, 1969.

[20] L. Rosenberg and S. Bocquet, "Non-coherent radar detection performance in medium grazing angle x-band sea clutter," *IEEE Transactions on Aerospace and Electronic Systems*, vol. 53, no. 2, pp. 669–682, 2017.

[21] P. Huang, S. Dong, X. Liu, X. Jiang, G. Liao, H. Xu, and S. Sun, "A coherent integration method for moving target detection using frequency agile radar," *IEEE Geoscience and Remote Sensing Letters*, vol. 16, no. 2, pp. 206–210, 2019.

[22] J. Zuk, S. Bocquet, and L. Rosenberg, "New saddle-point technique for non-coherent radar detection with application to correlated targets in uncorrelated clutter speckle," *IEEE Transactions on Signal Processing*, vol. 67, no. 8, pp. 2221–2233, 2019.

[23] S. Liu, Y. Cao, T.-S. Yeo, W. Wu, and Y. Liu, "Adaptive clutter suppression in randomized stepped-frequency radar," *IEEE Transactions on Aerospace and Electronic Systems*, vol. 57, no. 2, pp. 1317–1333, 2021.

[24] IEEE, "Recommended practice for radar cross-section test procedures," *IEEE Std 1502-2020 (Revision of IEEE Std 1502-2007)*, pp. 1–78, 2020.

[25] A. De Maio, M. Maffei, A. Aubry, and A. Farina, "Effects of plasma media with weak scintillation on the detection performance of space-borne radars," *IEEE Transactions on Geoscience and Remote Sensing*, vol. 60, pp. 1–13, 2022.

[26] D. A. Shnidman, "Radar detection probabilities and their calculation," *IEEE Transactions on Aerospace and Electronic Systems*, vol. 31, no. 3, pp. 928–950, 1995.

[27] R. D'Agostino and M. Stephens, *Goodness-of-Fit Techniques*. New York: Marcel Dekker, 1986.

[28] J. A. Nelder and R. Mead, "A simplex method for function minimization," *The computer journal*, vol. 7, no. 4, pp. 308–313, 1965.

[29] W. W. Daniel, *Applied Nonparametric Statistics*, ser. Duxbury advanced series in statistics and decision sciences. PWS-KENT Pub., 1990.
[30] G. Cui, A. De Maio, and M. Piezzo, "Performance prediction of the incoherent radar detector for correlated generalized swerling-chi fluctuating targets," *IEEE Transactions on Aerospace and Electronic Systems*, vol. 49, no. 1, pp. 356–368, 2013.
[31] M. Rosamilia, A. Aubry, A. Balleri, V. Carotenuto, and A. De Maio, "RCS measurements of UAVs and their statistical analysis," in *2022 IEEE 9th International Workshop on Metrology for AeroSpace (MetroAeroSpace)*, 2022, pp. 179–184.
[32] C. E. Brown, "Coefficient of variation," in *Applied multivariate statistics in geohydrology and related sciences*. Springer, 1998, pp. 155–157.
[33] D. G. Bonett, "Confidence interval for a coefficient of quartile variation," *Computational statistics & data analysis*, vol. 50, no. 11, pp. 2953–2957, 2006.
[34] E. F. Knott, J. F. Schaeffer, and M. T. Tulley, *Radar Cross Section*, ser. Radar, Sonar and Navigation. Institution of Engineering and Technology, 2004.
[35] D. P. Meyer and H. A. Mayer, "Radar target detection- handbook of theory and practice," *New York, Academic Press, Inc., 1973. 508 p*, 1973.
[36] P. Swerling, "Probability of detection for fluctuating targets," *IRE Transactions on Information Theory*, vol. 6, no. 2, pp. 269–308, 1960.